Fermi National Accelerator Laboratory

FERMILAB-Pub-00/049-T

Neutrino Oscillations at an Entry-Level Neutrino Factory and Beyond

V. Barger et al.

Fermi National Accelerator Laboratory
P.O. Box 500, Batavia, Illinois 60510

March 2000

Submitted to *Physical Review D*

Operated by Universities Research Association Inc. under Contract No. DE-AC02-76CH03000 with the United States Department of Energy

Fermilab-PUB 00/049-T
MADPH-00-1160
AMES-HET 00-01
March 2000

Neutrino Oscillations at an Entry-Level Neutrino Factory and Beyond

V. Barger[1], S. Geer[2], R. Raja[2], and K. Whisnant[3]

[1]*Department of Physics, University of Wisconsin, Madison, WI 53706, USA*
[2]*Fermi National Accelerator Laboratory, P.O. Box 500, Batavia, IL 60510, USA*
[3]*Department of Physics and Astronomy, Iowa State University, Ames, IA 50011, USA*

Abstract

We consider the parameters of an entry-level neutrino factory designed to make the first observation of $\nu_e \to \nu_\mu$ oscillations, measure the corresponding amplitude $\sin^2 2\theta_{13}$, and determine the sign of the atmospheric-scale δm^2_{32} via matter effects. A 50 kt detector, a stored muon energy $E_\mu \geq 20$ GeV and 10^{19} muon decays would enable these goals to be met provided $\sin^2 2\theta_{13} > 0.01$. The determination of the sign of δm^2_{32} also requires a baseline $L \geq 2000$ km. An upgraded neutrino factory with $O(10^{20})$ decays would enable the first observation of $\nu_e \to \nu_\tau$ oscillations. With $O(10^{21})$ decays the effects of a large CP-phase could be measured in the case of the large angle matter oscillation solution to the solar neutrino anomaly. Our analysis includes a family of three-neutrino models that can account for the atmospheric and solar neutrino oscillation indications.

I. INTRODUCTION

The observation of a deficit of muon-neutrinos in atmospheric neutrino experiments [1,2] has paved the way for a new generation of experiments studying neutrino masses and mixing. The neutrino sector offers exceptional opportunities for studying some of the most fundamental issues in particle physics, such as the origin of masses and CP violation. A major advantage over the quark sector is that neutrino phenomena are free of the complications of strong interactions. A comprehensive knowledge of the neutrino mixing matrix may yield clues to the old puzzle of why there is more than one lepton family.

The SuperKamiokande (SuperK) collaboration [1] has found that the atmospheric neutrino deficit is dependent on L/E_ν, with greater suppression of the ν_μ flux with increasing L/E_ν. Moreover, the electron-neutrino rate is L/E_ν independent and consistent with the calculated ν_e flux. The natural interpretation of the atmospheric data is in terms of $\nu_\mu \to \nu_\tau$ oscillations, with maximal or near-maximal mixing and a neutrino mass-squared difference $\delta m^2_{\rm atm} \simeq 3 \times 10^{-3}\,{\rm eV}^2$.

There are other indications of neutrino oscillation phenomena at δm^2 values distinct from the $\delta m^2_{\rm atm}$ scale. A long-standing puzzle is the observed deficits of solar neutrinos [3] compared to the flux predictions of the Standard Solar Model [4]. There are four regions [5] of oscillation parameters $\delta m^2_{\rm solar}$, $\sin^2 2\theta_{\rm solar}$ that can accommodate the present solar data. Three of the solutions involve resonance enhancements [6–10] due to the coherent scattering of ν_e from the dense solar medium. The Large Angle Matter (LAM) solution has $\delta m^2_{\rm solar} \sim 3 \times 10^{-5}\,{\rm eV}^2$, the Small Angle Matter (SAM) solution has $\delta m^2_{\rm solar} \sim 5 \times 10^{-6}\,{\rm eV}^2$, and the Long Oscillation Wavelength (LOW) solution has $\delta m^2_{\rm solar} \sim 10^{-7}\,{\rm eV}^2$ and large mixing. Vacuum Oscillation (VO) solutions [11,12] have $\delta m^2 \sim 10^{-10}\,{\rm eV}^2$ and large mixing. The Sudbury Neutrino Observatory (SNO) experiment [13] in progress may be able to exclude some of these solar solutions.

In addition there is some evidence for $\nu_\mu \to \nu_e$ and $\bar\nu_\mu \to \bar\nu_e$ oscillations from an accelerator experiment (LSND) at Los Alamos [14]. The observed event rates correspond to $\sin^2 2\theta_{\rm LSND} \sim 10^{-2}$ with $\delta m^2_{\rm LSND} \sim 1\,{\rm eV}^2$; a sizeable range of δm^2 values above 0.1 eV^2 is actually allowed. The mini-BooNE experiment at Fermilab [15], scheduled to start running in 2003, will determine whether the LSND effect is real.

In the next phase of neutrino oscillation studies long-baseline experiments are expected to confirm the $\nu_\mu \to \nu_\mu$ disappearance oscillations at the $\delta m^2_{\rm atm}$ scale. The K2K experiment [16] from KEK to SuperK, with a baseline of $L \simeq 250$ km and a mean neutrino energy of $\langle E_\nu \rangle \sim 1.4$ GeV is underway. The MINOS experiment from Fermilab to Soudan [17], with a longer baseline $L \simeq 730$ km and higher mean energies $\langle E_\nu \rangle = 3$, 6 or 12 GeV, is under construction and the ICANOE [18] and OPERA [19] experiments, with similar baselines from CERN to Gran Sasso, have been approved. These experiments with dominant ν_μ and $\bar\nu_\mu$ beams will securely establish the oscillation phenomena and may measure $\delta m^2_{\rm atm}$ to a precision of order 10% [20].

Further exploration of the neutrino mixing and mass-squared parameter space will require higher intensity neutrino beams and ν_e, $\bar\nu_e$ beams along with ν_μ, $\bar\nu_\mu$. To provide these neutrino beams, muon storage rings have been proposed [21,22] in which the muons decay in a long straight neutrino beam-forming section, and the muons are produced by a muon-collider type muon source [23]. These "neutrino factories" are now under serious

consideration [21–30]. The resulting neutrino beams would be sufficiently intense to produce thousands of oscillation events in a reasonably sized detector (10–50 kt) at distances up to the Earth's diameter [22]. Some initial studies have been made of the physics capabilities of such machines [24–30] as a function of the stored muon energy E_μ, baseline L, and intensity I. The focus of the present paper is how to best choose E_μ, L and I to maximize the physics output at an entry-level neutrino factory (hereafter referred to as ENuF) and beyond.

The present work expands on previous studies in several ways. First, we consider the *minimal* E_μ and I needed to accomplish our physics goals. Second, we consider the consequences of a number of model scenarios that can accommodate the atmospheric and solar oscillation indications. Third, we investigate possibilities for measuring CP-violating phases [24,29,31–34,36]. Finally, we investigate possibilities for observing $\nu_e \to \nu_\tau$ oscillations.

II. THEORETICAL OVERVIEW

A. Oscillation Formalism

The neutrino flavor eigenstates ν_α are related to the mass eigenstates ν_j in vacuum by a unitary matrix U,

$$|\nu_\alpha\rangle = \sum_j U_{\alpha j} \, |\nu_j\rangle \ . \tag{1}$$

The effect of matter on ν_e beams [7–10,30,37–39] has important consequences for long-baseline experiments. The propagation through matter is described by the evolution equation

$$i\frac{d\,|\nu_\alpha\rangle}{dx} = \sum_\beta \sum_{j\neq 1} \frac{1}{2E_\nu} \left[\delta m^2_{j1} U_{\alpha j} U^*_{\beta j} + A\delta_{\alpha e}\delta_{\beta e}\right] |\nu_\beta\rangle \ , \tag{2}$$

where $x = ct$ and $A/(2E_\nu)$ is the amplitude for coherent scattering of ν_e on electrons, and

$$A = 2\sqrt{2}\, G_F\, Y_e \rho E_\nu = 1.52 \times 10^{-4}\, \mathrm{eV}^2\, Y_e\, \rho\,(\mathrm{g/cm}^3) E\,(\mathrm{GeV})\,. \tag{3}$$

Here $Y_e(x)$ is the electron fraction and $\rho(x)$ is the matter density. The neutrino oscillation probabilities are then $P(\nu_\alpha \to \nu_\beta) = |\,\langle \nu_\beta(x = L) \mid \nu_\alpha(x = 0)\rangle\,|^2$.

We solve this evolution equation numerically taking into account the x-dependence of the density using the Preliminary Reference Earth model [40]. We have found that for L less than about 3000 km (in which the entire neutrino path is in the upper mantle and the density is approximately constant), the results of the exact propagation and those obtained assuming constant density agree to within a few percent. However, for larger L (where the neutrino path partially traverses the lower mantle and the density is no longer nearly constant) the assumption of constant density is no longer valid. For example, for $L = 7332$ km (the Fermilab to Gran Sasso distance), event rate predictions assuming constant density can be wrong by as much as 40%. We always use the numerical solution of Eq. (2) in our calculations.

For three neutrinos (with $\alpha = e, \mu, \tau$ and $j = 1, 2, 3$) the Maki-Nakagawa-Sakata (MNS) [41] mixing matrix will be parameterized by

$$U = \begin{pmatrix} c_{13}c_{12} & c_{13}s_{12} & s_{13}e^{-i\delta} \\ -c_{23}s_{12} - s_{13}s_{23}c_{12}e^{i\delta} & c_{23}c_{12} - s_{13}s_{23}s_{12}e^{i\delta} & c_{13}s_{23} \\ s_{23}s_{12} - s_{13}c_{23}c_{12}e^{i\delta} & -s_{23}c_{12} - s_{13}c_{23}s_{12}e^{i\delta} & c_{13}c_{23} \end{pmatrix}, \tag{4}$$

where $c_{jk} \equiv \cos\theta_{jk}$, $s_{jk} \equiv \sin\theta_{jk}$, and δ is the non-conserving phase. Two additional diagonal phases are present in U for Majorana neutrinos, but these do not affect oscillation probabilities.

B. Measuring θ_{13} and the Sign of δm^2_{32}

The oscillation channels $\nu_e \to \nu_\mu$ and $\bar{\nu}_e \to \bar{\nu}_\mu$ can be explored for the first time at a neutrino factory. In addition to a first observation of these transitions, the mixing angle θ_{13} can be measured, the sign of $\delta m^2_{\rm atm}$ can be determined from matter effects, and the CP phase δ could be measured or bounded. With this information, models of oscillation phenomena can be tested and discriminated.

The charged current (CC) interactions resulting from $\nu_e \to \nu_\mu$ and $\bar{\nu}_e \to \bar{\nu}_\mu$ oscillations produce "wrong-sign" muons (muons of opposite charge from the neutrinos in the beam). In the leading oscillation approximation the probability for $\nu_e \to \nu_\mu$ in 3-neutrino oscillations through matter of constant density is [7,37,38]

$$P(\nu_e \to \nu_\mu) = s^2_{23} \sin^2 2\theta^m_{13} \sin^2 \Delta^m_{32}\,, \tag{5}$$

where

$$\sin^2 2\theta^m_{13} = \frac{\sin^2 2\theta_{13}}{\left(\frac{A}{\delta m^2_{32}} - \cos 2\theta_{13}\right)^2 + \sin^2 2\theta_{13}} \tag{6}$$

and

$$\Delta^m_{32} = \frac{1.27 \delta m^2_{32}\,(\mathrm{eV}^2)\, L\,(\mathrm{km})}{E_\nu\,(\mathrm{GeV})} \sqrt{\left(\frac{A}{\delta m^2_{32}} - \cos 2\theta_{13}\right)^2 + \sin^2 2\theta_{13}}\,. \tag{7}$$

Here A is the matter amplitude of Eq. (3). Thus even with matter effects the $\nu_e \to \nu_\mu$ probability is approximately proportional to $\sin^2 2\theta_{13}$. The experimental sensitivity of the $\nu_e \to \nu_\mu$ measurements therefore changes almost linearly with $\sin^2 2\theta_{13}$.

For $\bar{\nu}_e \to \bar{\nu}_\mu$ oscillations, the sign of A is reversed in Eqs. (6) and (7). For $\sin^2 2\theta_{13} \ll 1$ and $A \sim \delta m^2_{32} > 0$, $P(\nu_e \to \nu_\mu)$ is enhanced and $P(\bar{\nu}_e \to \bar{\nu}_\mu)$ is suppressed by matter effects; the converse is the case for $-A \sim \delta m^2_{32} < 0$. Thus a comparison of the $\nu_e \to \nu_\mu$ and $\bar{\nu}_e \to \bar{\nu}_\mu$ CC rates gives information on the sign of δm^2_{32}.

C. $\nu_e \to \nu_\tau$ oscillations

The availability of ν_e and $\bar{\nu}_e$ beams from a neutrino factory would allow a search for $\nu_e \to \nu_\tau$ oscillations. In the leading oscillation approximation the probability for $\nu_e \to \nu_\tau$ oscillations through matter of constant density is [7,37,38]

$$P(\nu_e \to \nu_\tau) = c^2_{23} \sin^2 2\theta^m_{13} \sin^2 \Delta^m_{32}\,, \tag{8}$$

Thus the $\nu_e \to \nu_\tau$ probability in matter is also approximately proportional to $\sin^2 2\theta_{13}$.

D. CP Violation

In vacuum, CP violation in the lepton sector can be explored by comparing oscillation probabilities involving neutrinos with the corresponding probabilities for oscillations involving antineutrinos. For three-neutrino oscillations in a vacuum, the probability difference is

$$P(\nu_\alpha \to \nu_\beta) - P(\bar{\nu}_\alpha \to \bar{\nu}_\beta) = \mp 4J(\sin 2\Delta_{32} + \sin 2\Delta_{21} + \sin 2\Delta_{13}) \,, \tag{9}$$

where $\Delta_{jk} \equiv 1.27\delta m^2_{jk}(\mathrm{eV}^2)L(\mathrm{km})/E_\nu(\mathrm{GeV})$ and J is the CP-violating invariant [42,43], which can be defined as $J = Im\{U_{e2}U^*_{e3}U^*_{\mu 2}U_{\mu 3}\}$. The minus (plus) sign in Eq. (9) is used when α and β are in cyclic (anticyclic) order, where cyclic order is defined as $e\mu\tau$. For the mixing matrix in Eq. (4),

$$J = \frac{1}{8}\sin 2\theta_{12}\sin 2\theta_{13}\sin 2\theta_{23}\cos\theta_{13}\sin\delta \,. \tag{10}$$

Thus even for $\delta = \pm 90°$, J will be small when the $\theta_{12}\,, \theta_{13}$ mixing angles are small.

For $|\delta m^2_{32}| \gg |\delta m^2_{21}|$, the CP-violating probability difference for $\nu_e \to \nu_\mu$ is given approximately by

$$P(\nu_e \to \nu_\mu) - P(\bar{\nu}_e \to \bar{\nu}_\mu) \simeq -4J \sin\left(\frac{2.54\delta m^2_{21}(\mathrm{eV}^2)L(\mathrm{km})}{E_\nu(\mathrm{GeV})}\right) \,, \tag{11}$$

It is evident from Eq. (11) that CP violation is only appreciable in vacuum when the subleading oscillations (in this case oscillations due to δm^2_{21}) begin to develop [32]. The same qualitative results are expected when neutrinos propagate through matter, although the oscillation probabilities are changed.

III. FAMILY OF SCENARIOS

With three neutrinos, there are only two distinct δm^2 values. The evidence for atmospheric, solar and accelerator neutrino oscillations at three different δm^2 scales cannot be simultaneously accommodated in a three-neutrino framework. Here we set the accelerator evidence aside and use three-neutrino oscillations to explain atmospheric and solar data; the oscillation scale of the accelerator data is more relevant to short-baseline experiments.

TABLE I. Representative neutrino oscillation scenarios.

Scenario	$\lvert\delta m^2_{32}\rvert$ (atmos)	$\lvert\delta m^2_{21}\rvert$ (solar)	$\sin^2 2\theta_{23}$ (atmos)	$\sin^2 2\theta_{12}$ (solar)	$\sin^2 2\theta_{13}$	$J/\sin\delta$
1) LAM	3.5×10^{-3}	5×10^{-5}	1	0.8	0.04	0.022
2) SAM	3.5×10^{-3}	10^{-5}	1	0.01	0.04	0.0025
3) LOW	3.5×10^{-3}	10^{-7}	1	0.9	0.04	0.024
4) BIMAX	3.5×10^{-3}	5×10^{-5}	1	1	0	0

A family of representative scenarios in Table I, defined in the ongoing Fermilab long-baseline workshop study [44], will be adopted for our subsequent analysis; the central value

$|\delta m^2_{32}| = 3.5 \times 10^{-3}\,\mathrm{eV}^2$ is based on the published SuperK data [1]. With further data accumulation, a slightly lower central value of $2.8\times10^{-3}\,\mathrm{eV}^2$ is indicated [45], with a 90% C.L. range of $2-5\times10^{-3}$ eV^2. The forms of the mixing matrix U in these scenarios are

$$U(\mathrm{LAM}) = \begin{pmatrix} 0.846 & 0.523 & 0.101e^{-i\delta} \\ -0.372-0.060e^{i\delta} & 0.602-0.037e^{i\delta} & 0.704 \\ 0.372-0.060e^{i\delta} & -0.602-0.037e^{i\delta} & 0.704 \end{pmatrix}, \tag{12}$$

$$U(\mathrm{SAM}) = \begin{pmatrix} 0.994 & 0.050 & 0.101e^{-i\delta} \\ -0.035-0.071e^{i\delta} & 0.706-0.004e^{i\delta} & 0.704 \\ 0.035-0.071e^{i\delta} & -0.706-0.004e^{i\delta} & 0.704 \end{pmatrix}, \tag{13}$$

$$U(\mathrm{LOW}) = \begin{pmatrix} 0.807 & 0.582 & 0.101e^{-i\delta} \\ -0.413-0.058e^{i\delta} & 0.574-0.042e^{i\delta} & 0.704 \\ 0.413-0.058e^{i\delta} & -0.574-0.042e^{i\delta} & 0.704 \end{pmatrix}, \tag{14}$$

$$U(\mathrm{BIMAX}) = \begin{pmatrix} \frac{1}{\sqrt{2}} & \frac{1}{\sqrt{2}} & 0 \\ -\frac{1}{2} & \frac{1}{2} & \frac{1}{\sqrt{2}} \\ \frac{1}{2} & -\frac{1}{2} & \frac{1}{\sqrt{2}} \end{pmatrix}. \tag{15}$$

Since $\sin^2 2\theta_{13}$ is not well-known, sometimes we will consider the LAM solution with $\sin^2 2\theta_{13} = 0.004$, for which

$$U(\mathrm{LAM}') = \begin{pmatrix} 0.850 & 0.525 & 0.032e^{-i\delta} \\ -0.372-0.019e^{i\delta} & 0.602-0.012e^{i\delta} & 0.707 \\ 0.372-0.019e^{i\delta} & -0.602-0.012e^{i\delta} & 0.707 \end{pmatrix}. \tag{16}$$

Scenarios 1–3 in Table I represent three-neutrino oscillation explanations of the atmospheric and solar deficits, with the LAM, SAM, and LOW solar options, respectively. We do not address the VO solar solution separately, since the sub-leading δm^2 effects will not be significant and the LOW and VO scenarios will be indistinguishable. Scenario 4 with bimaximal atmospheric and LAM mixing [46] is interesting because the leading oscillation decouples in the $\nu_e \to \nu_\mu$ channel ($U_{e3} = 0$) and the sub-leading oscillations will therefore be more visible. However, in this scenario there are no matter effects on ν_e propagation and the sign of δm^2 cannot be so measured; also CP will be conserved.

The size of the Jarlskog invariant (modulo $\sin\delta$) is also shown in Table I; it is largest for the LAM and LOW scenarios (which have only one small angle), smaller for SAM (which has two small angles), and vanishes for the BIMAX scenario (in which one angle is zero). Since the observability of CP violation depends on both J *and* the size of the sub-leading oscillation scale δm^2_{21} (see Eq. (11)), one expects appreciable CP violation only in the LAM scenario.

The neutrino mass ordering can in principle be determined by the effects of matter on the leading electron neutrino oscillation [28]. To illustrate this, Fig. 1 shows the two possible three-neutrino mass patterns. Figure 1a, with one large mass m_3, has atmospheric neutrino oscillations with $\delta m^2_{32} > 0$. Figure 1b, with two large masses m_2, m_1, has $\delta m^2_{32} < 0$. For scenario 4, with no ν_e participation in the leading oscillations, there are no matter effects at the δm^2_{32} scale to determine the sign of δm^2_{32}.

IV. AN ENTRY-LEVEL NEUTRINO FACTORY

Neutrino factories require the development of new accelerator sub-systems which are technically challenging. The R&D required for a full-intensity muon source might take many years. It is reasonable to consider a strategy in which the R&D needed for the first neutrino factory is minimized by building, as a first step, a muon source that provides just enough muon decays per year to make contact with the interesting physics. If we also wish to minimize the cost of an entry-level facility, we must minimize the muon acceleration system and hence the energy of the muons decaying within the storage ring. In this section we consider, within the framework of the scenarios listed in Table I, the minimum muon energy and beam intensity needed at an ENuF.

We begin by defining our entry-level physics goal. We take this to be the first observation of $\nu_e \to \nu_\mu$ oscillations at the 10 event per year level. The signal will be the appearance of CC interactions which are tagged by a wrong-sign muon. To identify signal events we must be able to identify muons and measure their charge in the presence of the accompanying hadronic shower from the remnants of the target nucleon. Muons can only be cleanly identified and measured if their energy exceeds a threshold $E_{\rm min}$, which in practice is expected [47] to be a few GeV. This places an effective lower bound on the acceptable energy of the muon storage ring. To illustrate this, consider the $\nu_e \to \nu_\mu$ signal in a detector that is 2800 km downstream of a 20 GeV neutrino factory. The predicted measured energy distributions for CC events tagged by wrong-sign muons are shown for the LAM scenario (Table I) in Fig. 2 as a function of $E_{\rm min}$. As $E_{\rm min}$ increases the signal efficiency decreases. For example, with $E_{\rm min} =$ 2 (4) [6] GeV the resulting signal loss is 18% (36%) [55%]. In addition, as $E_{\rm min}$ increases the measured signal distributions become increasingly biased towards higher energies, and the information on the oscillations encoded in the energy distribution is lost. We conclude from Fig. 2 that with a 20 GeV storage ring we can probably tolerate an $E_{\rm min}$ of a few GeV, but would not want to decrease the storage ring energy below 20 GeV. Hence, we will adopt 20 GeV as the minimum storage ring energy for an ENuF. In the following, our calculations include a muon threshold $E_{\rm min} = 4$ GeV, and for simplicity we assume the detection efficiency is 0 for signal events with $E_\mu < E_{\rm min}$ and 1 for $E_\mu > E_{\rm min}$.

We next consider the muon beam intensity required to meet our entry-level physics goal if the storage ring energy is 20 GeV. To minimize the required beam intensity we must maximize the detector mass (M). Recently 50 kt has been considered [47] as a plausible although ambitious M. We therefore choose $M = 50$ kt. In addition to the neutrino factory beam properties and the detector mass, the signal event rate will depend upon the baseline and the oscillation parameters. Since, to a good approximation, the signal rate is proportional to $\sin^2 2\theta_{13}$, it is useful to define the $\sin^2 2\theta_{13}$ "reach" for an experiment as the value of $\sin^2 2\theta_{13}$ for which our physics goal (in this case the observation of 10 signal events per year) will be met. Setting the number of useful muon decays per year to 10^{19}, the $\sin^2 2\theta_{13}$ reach is shown in Fig. 3 as a function of baseline and δm^2_{32} with the other oscillation parameters corresponding to the LAM scenario. The calculational methods are described in Ref. [27,28]. The $\sin^2 2\theta_{13}$ reach degrades slowly as L increases, and improves with increasing $|\delta m^2_{32}|$, varying by about a factor of 5 over the δm^2_{32} range currently favored by the SuperK results. Note that, for δm^2_{32} in the center of the SuperK range, our entry level goal would be met with a 20 GeV storage ring and 10^{19} decays per year provided $\sin^2 2\theta_{13}$

exceeds approximately 0.01, which is more than an order of magnitude below the currently excluded region.

We now consider how the muon beam intensity required to meet our entry-level physics goal varies with the storage ring energy. We will choose a baseline of 2800 km, motivated by a consideration of the physics sensitivity of an upgraded ENuF (see next section). The number of muon decays required to meet our goal is shown in Fig. 4 versus the muon storage ring energy for the LAM, SAM, LOW, and BIMAX oscillation scenarios. Note that:

(i) The energy dependent intensities needed for the SAM and LOW scenarios are indistinguishable.

(ii) Due to the contributions from sub-leading oscillations, the intensity needed for the LAM scenario is slightly less than needed for the SAM and LOW scenarios.

(iii) With a 20 GeV storage ring 2×10^{18} muon decays per year would meet our entry level physics goals for the LAM, SAM, and LOW scenarios. The dependence of the required muon intensity I on the storage ring energy is approximately given by $I \propto E^{-1.6}$.

(iv) For the BIMAX scenario in which $\sin^2 2\theta_{13} = 0$ only the sub-leading δm^2 scale contributes to the signal. With a 20 GeV storage ring a few $\times 10^{20}$ muon decays per year would be needed to observe $\nu_e \to \nu_\mu$ oscillations. Although this scenario would be bad news for a low-intensity neutrino factory, oscillations driven by the sub-leading δm^2 scale might be studied with a higher intensity muon source.

It is straightforward to use the curves in Fig. 4 to infer the intensity required to meet our entry level goals for LAM, SAM, and LOW-type scenarios with values of $\sin^2 2\theta_{13}$ other than 0.04. For example, if $\sin^2 2\theta_{13} = 0.01$ (a factor of 20 below the currently excluded value, and a factor of 4 below the value used for the curves in Fig. 4) we must multiply the beam intensity indicated in Fig. 4 by a factor of 4 to achieve our entry-level goal. Provided a 50 kt detector with good signal efficiency is practical, within the framework of LAM, SAM and LOW-type scenarios, a 20 GeV storage ring in which there are 10^{19} muon decays per year in the beam forming straight section would enable the first observation of $\nu_e \to \nu_\mu$ oscillations provided $\sin^2 2\theta_{13} > 0.01$.

Consider next the prospects for exploiting $\nu_e \to \nu_\mu$ measurements to determine the sign of δm^2_{32}. In ref. [28] we have shown in the LAM scenario that the sign of δm^2_{32} can be determined by comparing the wrong-sign muon rates and/or the associated CC event energy distributions when respectively positive and negative muons are stored in the ring. The most sensitive technique to discriminate $\delta m^2_{32} > 0$ from $\delta m^2_{32} < 0$ would be to take data when there were alternately positive and negative muons stored in the neutrino factory, and measure the resulting wrong-sign muon event energy distributions together with the $\nu_\mu \to \nu_\mu$ and $\overline{\nu}_\mu \to \overline{\nu}_\mu$ event energy distributions. The four distributions can then be simultaneously fit with the oscillation parameters δm^2_{32} (including its sign), $\sin^2 2\theta_{13}$, and $\sin^2 2\theta_{23}$ left as free parameters [48]. In the following we take a simpler approach to demonstrate that, provided L is large enough, a neutrino factory that permitted the observation of 10 $\nu_e \to \nu_\mu$ events per year would also enable the sign of δm^2_{32} to be determined.

We begin by defining the ratio:

$$R_{e\mu} = \frac{N(\bar{\nu}_e \to \bar{\nu}_\mu)}{N(\nu_e \to \nu_\mu)} \tag{17}$$

$R_{e\mu}$ is just the ratio of wrong-sign muon rates when respectively negative and positive muons are stored in the neutrino factory. Figure 5 shows $R_{e\mu}$ as a function of L for $E_\mu = 20$ GeV and $\delta m^2_{32} = \pm 3.5 \times 10^{-3}$ eV^2/c^4. Note that when $L > 2000$ km the ratio $R_{e\mu}$ for positive δm^2_{32} is more than a factor of 5 greater than the value for negative δm^2_{32}. As an example, consider a 50 kt detector 2800 km downstream of a 20 GeV storage ring in which there are 10^{19} muon decays per year in the beam forming straight section. Suppose that $\sin^2 2\theta_{13} = 0.01$, and assume we know that $|\delta m^2_{32}| \sim 3.5 \times 10^{-3}$ eV^2/c^4 from $\nu_\mu \to \nu_\mu$ measurements, for example. If we store positive muons in the neutrino factory after one year we would expect to observe 11 wrong-sign muon events if $\delta m^2_{32} > 0$ but only 2 events if $\delta m^2_{32} < 0$. To reduce the uncertainties due to the lack of precise knowledge of the other oscillation parameters, we can then take data with negative muons stored. We would then expect to observe less than 2 wrong-sign muon events per year if $\delta m^2_{32} > 0$, but 6 events per year if $\delta m^2_{32} < 0$. Clearly with these statistics and several years of data taking the sign of δm^2_{32} could be established. From this example we conclude that with a few years of data taking a neutrino factory that enabled the observation of 10 $\nu_\mu \to \nu_\mu$ events per year would also enable the sign of δm^2_{32} to be determined provided the baseline was sufficiently long ($L > 2000$ km) so that the prediction for $R_{e\mu}$ changes by a large factor (> 5) when the assumed sign of δm^2_{32} is changed. Hence, provided $\sin^2 2\theta_{13} > 0.01$, our entry-level neutrino factory would make the first observation of $\nu_\mu \to \nu_\mu$ oscillations, measure $\sin^2 2\theta_{13}$, and determine the pattern of neutrino masses.

V. ONE STEP BEYOND AN ENTRY LEVEL NEUTRINO FACTORY

An entry-level neutrino factory is attractive if there is a beam intensity and/or energy upgrade path that enables a more comprehensive physics program beyond the initial observation of $\nu_e \to \nu_\mu$ oscillations and determination of the sign of δm^2_{32}. In this section we consider the energy and/or intensity upgrades needed to achieve a reasonable upgrade physics goal, which we take to be the first observation of $\nu_e \to \nu_\tau$ oscillations.

In ref. [27] we have shown that in a LAM-like scenario the $\nu_e \to \nu_\tau$ oscillation event rates in a multi-kt detector are expected to be significant if E_μ is 20 GeV or greater. In the following we consider the neutrino factory beam energy and intensity needed to make a first observation of $\nu_e \to \nu_\tau$ oscillations at the 10 event level in one year of running with a fully efficient detector (or several years with a realistic detector). Our detector must be able to measure τ appearance and, to separate the signal from $\nu_\mu \to \nu_\tau$ oscillation backgrounds, measure the sign of the charge of the τ. Hybrid emulsion detectors in an external magnetic field provide an example of a candidate detector technology that might be used. Consideration of detector technologies and their performance is under study [49], and is outside the scope of the present paper. We will take $M = 5$ kt as a plausible, but aggressive, choice for the detector mass.

Consider first an intensity-upgraded ENuF, namely a 20 GeV storage ring in which there are 10^{20} muon decays per year in the beam forming straight section. The τ appearance rates from $\nu_e \to \nu_\tau$ and $\nu_\mu \to \nu_\tau$ oscillations are shown as a function of $\sin^2 2\theta_{13}$ and δm^2_{32} in Fig. 6

for a 5 kt detector at $L = 2800$ km. In contrast to the $\nu_\mu \to \nu_\tau$ background rate, which is independent of $\sin^2 2\theta_{13}$, the $\nu_e \to \nu_\tau$ signal rate increases linearly with $\sin^2 2\theta_{13}$. Note that for the LAM scenario with $\sin^2 2\theta_{13} = 0.04$ and $\delta m^2_{32} = 0.0035$ eV^2, there are about 10 signal events per $10^{20}\mu^+$ decays, and 300 $\nu_\mu \to \nu_\tau$ background events. Thus it is desirable that the τ sign mis-determination be less than of order 1 in 300.

Next consider the dependence of the $\sin^2 2\theta_{13}$ reach (for detecting 10 $\nu_e \to \nu_\tau$ events) on L and the storage ring energy. Fixing $\delta m^2_{32} = 0.0035$ eV^2, the $\sin^2 2\theta_{13}$ reach is shown in Fig. 7 to improve with energy, and to be almost independent of L over the range considered except at the highest energies and longest baselines, for which the reach is degraded. For $L \sim 3000$ km, an energy upgrade from 20 GeV to 50 GeV would improve the reach by about a factor of 5. The energy dependence of the muon intensity required to meet our $\nu_e \to \nu_\tau$ discovery goal is summarized in Fig. 4. We conclude that a neutrino factory consisting of a 20 GeV storage ring in which there are 10^{20} muon decays per year in the beam forming straight section would enable the first observation of $\nu_e \to \nu_\tau$ oscillations in LAM, SAM, and LOW-type scenarios with $\sin^2 2\theta_{13} > 0.01$ provided a 5 kt detector with good τ signal efficiency and charge-sign determination is practical.

VI. MEASURING THE CP NON-CONSERVING PHASE

In the event that the solar solution is LAM, CP non-conserving effects may be large enough to allow a measurement of the MNS phase δ at a high-intensity neutrino factory [24,29,35]. The total rate of appearance events very strongly depends on the value of $\sin^2 2\theta_{13}$. For example, Figs. 8 and 9 show the event rates versus L for the LAM solution in Table I with $\delta = 0$ and $\sin^2 2\theta_{13} = 0.04$, 0.004, and 0. For L less than about 5000 km the event rates for the BIMAX solution are about 25% higher than the $\sin^2 2\theta_{13} = 0$ curve. Although the rates decrease significantly with decreasing $\sin^2 2\theta_{13}$, even for $\sin^2 2\theta_{13} = 0$ there is a residual signal from the sub-leading oscillation in the LAM scenario which may be detectable.

Figures 5, 10, and 11 show predictions for the CP dependent ratio $R_{e\mu}$ versus the baseline L for a 50 kt detector in the LAM scenario with $\delta m^2_{32} = 3.5 \times 10^{-3}$ eV^2. The error bars are representative statistical uncertainties. These figures present the results of calculations with decays/year and $\sin^2 2\theta_{13}$ values of (10^{20}, 0.04), (10^{21}, 0.04), and (10^{21}, 0.004), respectively. Results for phases $\delta = 0°$, $\delta = 90°$, and $\delta = -90°$ are shown in each case, for both positive and negative values of δm^2_{32}. For these values of $\sin^2 2\theta_{13}$ the event rates show a strong dependence on the sign of δm^2_{32} (due to different matter effects for neutrinos and antineutrinos), and a smaller dependence on the CP-violating phase. Figure 12 shows the results for 10^{21} muons and $\sin^2 2\theta_{13} = 0.04$ in finer detail. Note that at small distances $R_{e\mu}$ is not unity for $\delta = 0$ (even though matter effects are small) because the $\bar{\nu}_\mu$ and ν_μ CC cross sections are different. We note that the CP-violating effect is largest in the range $L \simeq$ 2000–3000 km, vanishes for $L \simeq 7000$ km, and is nonzero but with large uncertainties for $L > 7000$ km.

Similar calculations show that for the SAM and LOW model parameters $R_{e\mu}$ is essentially independent of δ, verifying the conclusions of Sec. III that CP violation is negligible in these scenarios. The effect of matter in the SAM and LOW scenarios, which depends on the sign of δm^2_{32} and the size of $\sin^2 2\theta_{13}$, is similar to the LAM case.

A nonzero $\sin^2 2\theta_{13}$ is needed both to determine the sign of δm^2_{32} via matter effects, and to have observable CP violation from the sub-leading scale; however, whether matter or CP violation gives the largest effect depends on the size of $\sin^2 2\theta_{13}$. This is illustrated in Fig. 13, which shows the ratio of wrong sign muon events versus $\sin^2 2\theta_{13}$ for our representative LAM solar solution with 10^{21} muons/year. For larger values of $\sin^2 2\theta_{13}$, say above about 0.001, the sign of δm^2_{32} (through matter effects) has the largest effect on the ratio, while for $\sin^2 2\theta_{13} < 0.001$ the value of δ (which largely determines the amount of CP violation) has the largest effect.

Now consider the neutrino factory energy and intensity needed to begin to probe the CP phase δ in the LAM scenario. We will define the $\sin^2 2\theta_{13}$ reach as that value of $\sin^2 2\theta_{13}$ that (with a 50 kt detector and two years of data taking) will enable a 3σ discrimination between (a) $\delta = 0$ and $\delta = \pi/2$ and (b) $\delta = 0$ and $\delta = -\pi/2$. The measurement will be based on a comparison of wrong-sign muon rates when respectively positive and negative muons are alternately stored in the ring. The $\sin^2 2\theta_{13}$ reach when there are 10^{21} decays per year is shown for the 3σ discrimination between $\delta = 0$ and $\pm\pi/2$ in Fig. 14 as a function of baseline and stored muon energy. The optimum baseline is about 3000 km, for which the $\sin^2 2\theta_{13}$ reach is a little better (worse) than 0.01 for the $\delta = \pi/2$ ($\delta = -\pi/2$) discrimination, and is almost independent of muon energy over the range considered (Fig. 4). Thus, a high intensity 20 GeV neutrino factory providing O(10^{21}) muon decays per year might begin to probe CP violation in the lepton sector if the LAM scenario is the correct description of neutrino oscillations, and a 50 kt detector with good signal efficiency is practical. This conclusion is consistent with results presented in Ref. [29] in which global fits to the measured oscillation distributions have been studied to determine the precision with which δ and $\sin^2 2\theta_{13}$ can be simultaneously measured at a neutrino factory.

VII. SUMMARY

We briefly summarize the results of our study of the physics goals of an entry-level neutrino factory as follows:

(i) An entry-level machine would make a first observation of $\nu_e \to \nu_\mu$ oscillations, measure the corresponding amplitude $\sin^2 2\theta_{13}$, and determine the sign of δm^2_{32}.

(ii) The $\sin^2 2\theta_{13}$ reach for the first observation of $\nu_e \to \nu_\mu$ oscillations and the measurement of the sign of δm^2_{32} is insensitive to the solar neutrino oscillation solution (LAM, SAM, or LOW) within a 3-neutrino framework.

(iii) A 20 GeV neutrino factory providing 10^{19} muon decays per year would enable our entry-level physics goals to be met provided $\sin^2 2\theta_{13} > 0.01$ and a detector with good muon charge-sign determination and a mass of 50 kt is practical. The required beam intensity might be a factor of 2–3 higher or lower depending on where within the SuperK range the δm^2_{32} parameter sits. The event rates also depend on the muon energy detection threshold ($E_{\rm min} = 2$–5 GeV) and we win or lose a factor of 2 in rates depending on how low this threshold can be pushed. To determine the sign of δm^2_{32} a long baseline ($L > 2000$ km) must be chosen.

(iv) A candidate for an intensity-upgraded neutrino factory would be a 20 GeV facility providing 10^{20} muon decays per year. In addition to the precise determination of the oscillation parameters, the upgraded neutrino source would enable the first observation of $\nu_e \to \nu_\tau$ oscillations provided $\sin^2 2\theta_{13} > 0.01$ and a 5 kt detector with good τ signal efficiency and charge-sign determination is practical.

(v) With a high-intensity neutrino factory providing a few $\times 10^{20}$ muon decays per year, the ratio of μ^+/μ^- wrong-sign muon rates might enable detection of a maximal CP phase in the case of the LAM solar solution. If $\sin^2 2\theta_{13}$ is vanishingly small, (for example the bimaximal mixing scenario) a first observation of $\nu_e \to \nu_\mu$ oscillations at a high intensity neutrino factory might provide a direct measurement of oscillations driven by the sub-leading δm^2 scale, although wrong-sign muon backgrounds might be problematic.

In conclusion, the required number of muon decays per year to achieve the various physics goals of interest are summarized in Fig. 4. At a 20 GeV neutrino factory 10^{18}–10^{19} decays per year are required for a thorough search for $\nu_e \to \nu_\mu$ appearance, 10^{20} to observe $\nu_e \to \nu_\tau$ oscillations, and 10^{20}–10^{21} to probe the sub-leading oscillation scale and detect CP violation effects in a three-neutrino LAM model.

ACKNOWLEDGMENTS

This research was supported in part by the U.S. Department of Energy under Grant No. DE-FG02-95ER40896 and in part by the University of Wisconsin Research Committee with funds granted by the Wisconsin Alumni Research Foundation.

REFERENCES

[1] Super-Kamiokande Collaboration, Y. Fukuda et al., Phys. Lett. **B433**, 9 (1998); Phys. Lett. **B436**, 33 (1998); Phys. Rev. Lett. **81**, 1562 (1998); Phys. Rev. Lett. **82**, 2644 (1999).

[2] Kamiokande collaboration, K.S. Hirata *et al.*, Phys. Lett. **B280**, 146 (1992); Y. Fukuda *et al.*, Phys. Lett. **B335**, 237 (1994); IMB collaboration, R. Becker-Szendy *et al.*, Nucl. Phys. Proc. Suppl. **38B**, 331 (1995); Soudan-2 collaboration, W.W.M. Allison *et al.*, Phys. Lett. **B391**, 491 (1997); MACRO collaboration, M. Ambrosio *et al.*, Phys. Lett. **B434**, 451 (1998).

[3] B.T. Cleveland *et al.*, Nucl. Phys. B (Proc. Suppl.) **38**, 47 (1995); GALLEX collaboration, W. Hampel *et al.*, Phys. Lett. **B388**, 384 (1996); SAGE collaboration, J.N. Abdurashitov *et al.*, Phys. Rev. Lett. **77**, 4708 (1996); Kamiokande collaboration, Y. Fukuda *et al.*, Phys. Rev. Lett, **77**, 1683 (1996); Super-Kamiokande collaboration, Y. Fukuda *et al.*, Phys. Rev. Lett. **82**, 2430 (1999); Phys. Rev. Lett. **82**, 1810 (1999).

[4] J.N. Bahcall, S. Basu, and M.H. Pinsonneault, Phys. Lett. **B 433**, 1 (1998), and references therein.

[5] A. de Gouvea, A. Friedland, and H. Murayama, hep-ph/0002064; G.L. Fogli, E. Lisi, D. Mintanino, and A. Palazzo, hep-ph/9912231. M.C. Gonzalez-Garcia, P.C. de Holanda, C. Peña-Garay, and J.W.F. Valle, hep-ph/9906469; J.N. Bahcall, P. Krastev, and A.Yu. Smirnov, hep-ph/9905220; V. Barger and K. Whisnant, Phys. Lett. **456**, 54 (1999); V. Barger and K. Whisnant, Phys. Rev. **D59**, 093007 (1999); J.N. Bahcall, P. Krastev, and A.Yu. Smirnov, Phys. Rev. **D58**, 096016 (1998); R. Barbieri, L.J. Hall, D. Smith, A. Strumia, and N. Weiner, JHEP 9812, 017 (1998); N. Hata and P. Langacker, Phys. Rev. **D56**, 6107 (1997).

[6] L. Wolfenstein, Phys. Rev. **D17**, 2369 (1978).

[7] V. Barger, S. Pakvasa, R.J.N. Phillips, and K. Whisnant, Phys. Rev. **D22**, 2718 (1980).

[8] P. Langacker, J.P. Leveille, and J. Sheiman, Phys. Rev. **D 27**, 1228 (1983);

[9] S.P. Mikheyev and A. Smirnov, Yad. Fiz. **42**, 1441 (1985) [Sov. J. Nucl. Phys. 42, 913 (1986)].

[10] S. Parke, Phys. Rev. Lett. **57**l, 1275 (1986); S.P. Rosen and J.M. Gelb, Phys. Rev. **D34**, 969 (1986); W. Haxton, Phys. Rev. Lett. **56**, 1305 (1986).

[11] V. Barger, K. Whisnant, R.J.N. Phillips, Phys. Rev. **D24**, 538 (1981); S.L. Glashow and L.M. Krauss, Phys. Lett. **B190**, 199 (1987).

[12] V. Barger and K. Whisnant, Phys. Lett. **B456**, 54 (1999); V. Barger, R.J.N. Phillips, and K. Whisnant, Phys. Rev. Lett. **65**, 3084 (1990); **69**, 3135 (1992); P.I. Krastev and S.T. Petcov, Phys. Lett. **B 285**, 85 (1992); Nucl. Phys. **B449**, 605 (1995); S.L. Glashow, P.J. Kernan, and L.M. Krauss, Phys. Lett. **B445**, 412 (1999).

[13] G.T. Ewans et al., Physics in Canada **48**, 2 (1992); see also the SNO web pages at http://www.sno.phy.queensu.ca/

[14] C. Athanassopoulos et al. (LSND Collab.), Phys. Rev. Lett. **77**, 3082 (1996); Phys. Rev. Lett. **81**, 1774 (1998).

[15] E. Church et al. (BooNE Collab.), "A letter of intent for an experiment to measure $\nu_\mu \to \nu_e$ oscillations and ν_μ at the Fermilab Booster", May 16, 1997, unpublished.

[16] K. Nishikawa et al. (KEK-PS E362 Collab.), "Proposal for a Long Baseline Neutrino Oscillation Experiment, using KEK-PS and Super-Kamiokande", 1995, unpublished;

INS-924, April 1992, submitted to J. Phys. Soc. Jap.; Y. Oyama, Proc. of the YITP Workshop on Flavor Physics, Kyoto, Japan, 1998, hep-ex/9803014.
[17] MINOS Collaboration, "Neutrino Oscillation Physics at Fermilab: The NuMI-MINOS Project," NuMI-L-375, May 1998.
[18] See the ICANOE web page at http://pcnometh4.cern.ch/
[19] See the OPERA web page at http://www.cern.ch/opera/
[20] D. A. Petyt,"A study of parameter measurement in a long-baseline neutrino oscillation experiment", Thesis submitted to Univ. of Oxford, England, 1998.
[21] S. Geer, "Neutrino beams from muon storage rings: characteristics and physics potential", FERMILAB-PUB-97-389, 1997, presented at the Workshop on Physics at the First Muon Collider and Front-End of a Muon Collider, November, 1997.
[22] S. Geer, Phys. Rev. **D57**, 6989 (1998).
[23] C. Ankenbrandt et al. (Muon Collider Collaboration), Phys. Rev. ST Accel. Beams 2, 081001 (1999).
[24] A. De Rujula, M.B. Gavela, and P. Hernandez, Nucl. Phys. **B547**, 21 (1999).
[25] M. Campanelli, A. Bueno, and A. Rubbia, hep-ph/9905240.
[26] R.B. Palmer et al. (Muon Collider Collababoration), http://pubweb/bnl.gov/people/palmer/nu/params.ps
[27] V. Barger, S. Geer, and K. Whisnant, Phys. Rev. **D 61**, 053004 (2000).
[28] V. Barger, S. Geer, R. Raja, and K. Whisnant, hep-ph/9911524.
[29] A. Cervera, A. Donini, M.B. Gavela, J.J. Gomez Cadenas, P. Hernandez, O. Mena, and S. Rigolin, hep-ph/0002108.
[30] I. Mocioiu and R. Shrock, hep-ph/9910554, hep-ph/0002149.
[31] N. Cabbibo, Phys. Lett. **B72**, 333 (1978).
[32] V. Barger, K. Whisnant, R.J.N. Phillips, Phys. Rev. Lett. **45**, 2084 (1980)
[33] S. Pakvasa, in *Proc. of the XXth International Conference on High Energy Physics*, ed. by L. Durand and L.G. Pondrom, AIP Conf. Proc. No. 68 (AIP, New York, 1981), Vol. 2, p.
[34] V. Barger, Y.-B. Dai, K. Whisnant, and B.-L. Young, Phys. Rev. **D59**, 113010 (1999).
[35] M. Freund, M. Lindner, S.T. Petcov, and A. Romanino, hep-ph/9912457.
[36] For other recent discussions of CP violation effects in neutrino oscillations, see D.J. Wagner and T.J. Weiler, Phys. Rev. **D59**, 113007 (1999); A.M. Gago, V. Pleitez, R.Z. Funchal, hep-ph/9810505; K.R. Schubert, hep-ph/9902215; K. Dick, M. Freund, M. Lindner and A. Romanino, hep-ph/9903308; J. Bernabeu, hep-ph/9904474; S.M. Bilenky, C. Giunti, and W. Grimus, Phys. Rev. **D58**, 033001 (1998); M. Tanimoto, Prog. Theor. Phys. **97**, 901 (1997); J. Arafune, J. Sato, Phys. Rev. **D55**, 1653 (1997); T. Fukuyama, K. Matasuda, H. Nishiura, Phys. Rev. **D57**, 5844 (1998); M. Koike and J. Sato, hep-ph/9707203, Proc. of the KEK Meetings on CP Violation and its Origin; H. Minakata and H. Nunokawa, Phys. Lett. **B413**, 369 (1997); H. Minakata and H. Nunokawa, Phys. Rev. **D57**, 4403 (1998); J. Arafune, M. Koike and J. Sato, Phys. Rev. **D56**, 3093 (1997); M. Tanimoto, Phys. Lett. **B435**, 373 (1998).
[37] R. Bernstein and S. Parke, Phys. Rev. **D44**, 2069 (1991).
[38] J. Pantaleone, Phys. Rev. **D49**, 2152 (1994); Phys. Rev. Lett. **81**, 5060 (1998);
[39] P. Lipari, hep-ph/9903481; E. Akhmedov, P. Lipari, and M. Lusignoli, Phys. Lett. **B300**, 128 (1993); P. Lipari and M. Lusignoli, Phys. Rev. **D58**, 073005 (1998); E. Akhmedov, A. Dighe, P. Lipari, and A.Yu. Smirnov, Nucl. Phys. **B542**, 3 (1999); E.K. Akhmedov, Nucl. Phys. **B538**, 25 (1998); S.T. Petcov, Phys. Lett. **B434**, 321 (1998); M.V.

Chizhov, M. Maris, and S.T. Petcov, hep-ph/9810501; M.V. Chizhov and S.T. Petcov, hep-ph/9903424; S.T. Petcov, hep-ph/9910335; H.W. Zaglauer and K.H. Schwarzer, Z. Phys. **C40**, 273 (1988); Q. Liu, S. Mikheyev, and A.Yu. Smirnov, Phys. Lett. **B440**, 319 (1998); P.I. Krastev, Nuovo Cimento A **103**, 361 (1990). J. Pruet and G.M. Fuller, astro-ph/9904023. J. Arafune, J. Sato, Phys. Rev. **D55**, 1653 (1997); J. Arafune, M. Koike and J. Sato, Phys. Rev. **D56**, 3093 (1997); M. Tanimoto, Prog. Theor. Phys. **97**, 901 (1997); H. Minakata and H. Nunokawa, Phys. Lett. **B413**, 369 (1997); H. Minakata and H. Nunokawa, Phys. Rev. **D57**, 4403 (1998); M. Koike and J. Sato, hep-ph/9909469; M. Koike and J. Sato, hep-ph/9911258; T. Ohlsson and H. Snellman, hep-ph/9910546; A. Romanino, hep-ph/9909425.

[40] Parameters of the Preliminary Reference Earth Model are given by A. Dziewonski, Earth Structure, Global, in "The Encyclopedia of Solid Earth Geophysics", ed. by D.E. James, (Van Nostrand Reinhold, New York, 1989) p. 331; also see R. Gandhi, C. Quigg, M. Hall Reno, and I. Sarcevic, Astroparticle Physics **5**, 81 (1996).

[41] Z. Maki, M. Nakagawa, and S. Sakata, Prog. Theor. Phys. **28**, 870 (1962).

[42] W.-Y. Keung and L.-L. Chau, Phys. Rev. Lett. **53**, 1802 (1984).

[43] C. Jarlskog, Z. Phys. **C 29**, 491 (1985); Phys. Rev. **D 35**, 1685 (1987).

[44] See the Fermilab Long-Baseline Workshop web site at http://www.fnal.gov/projects/muon_collider/nu/study/study.html

[45] T. Kajita, talk presented at the *7th International Symposium on Particles, Strings and Cosmology (PASCOS 99)*, Granlibakken, CA, Dec. 1999, http://pc90.ucdavis.edu/talks/plenary/Kajita/

[46] V. Barger, S. Pakvasa, T.J. Weiler, and K. Whisnant, Phys. Lett. **B437** 107 (1998); A.J. Baltz, A.S. Goldhaber, and M. Goldhaber, Phys. Rev. Lett. **81**, 5730 (1998).

[47] Talks by P. Spentzouris, D. Harris, K. McFarland, D. Casper, M. Campanelli, and S. Rigolin at the two day neutrino factory physics study meeting, Fermilab, 17-18 February, 2000. See http://www.fnal.gov/projects/muon_collider/nu/study/study.html

[48] V. Barger, S. Geer, R. Raja, and K. Whisnant, in preparation.

[49] See http://www.fnal.gov/projects/muon_collider/nu/study/study.html

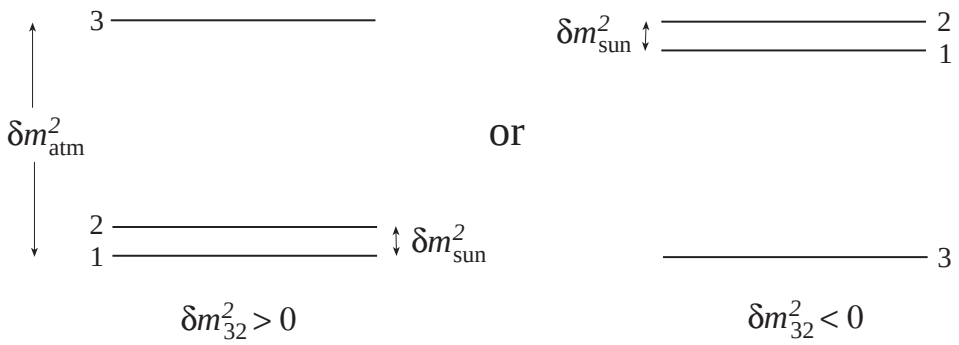

FIG. 1. Two patterns of three-neutrino mass spectra that can explain the atmospheric and solar neutrino anomalies: (a) $\delta m^2_{32} > 0$, (b) $\delta m^2_{32} < 0$.

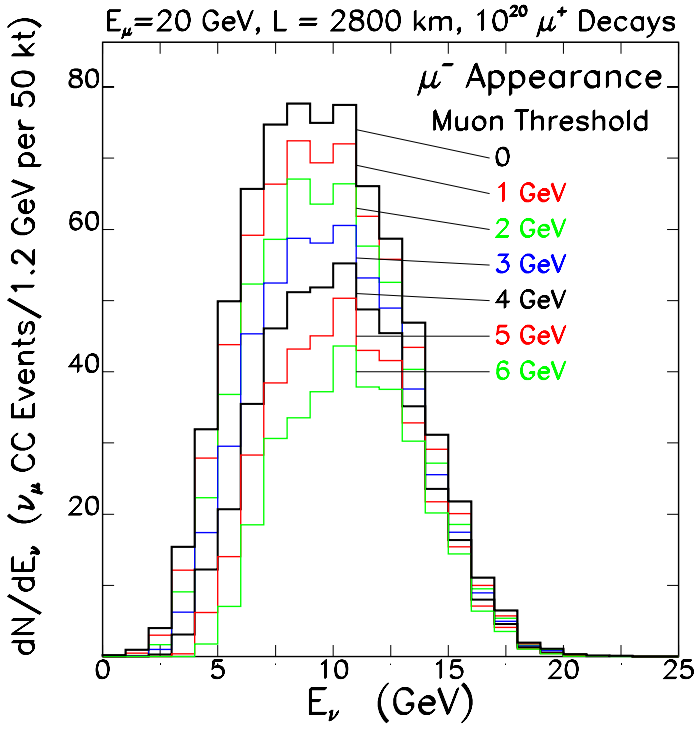

FIG. 2. Predicted measured energy distributions (including the detector resolution function) for $\nu_e \to \nu_\mu$ CC events tagged by wrong-sign muons when 20 GeV positive muons are stored in the neutrino factory and a 50 kt detector is at $L = 2800$ km. The distributions are shown for a variety of muon detection threshold energies $E_{\rm min}$. The oscillation parameters are those for the LAM scenario (Table I).

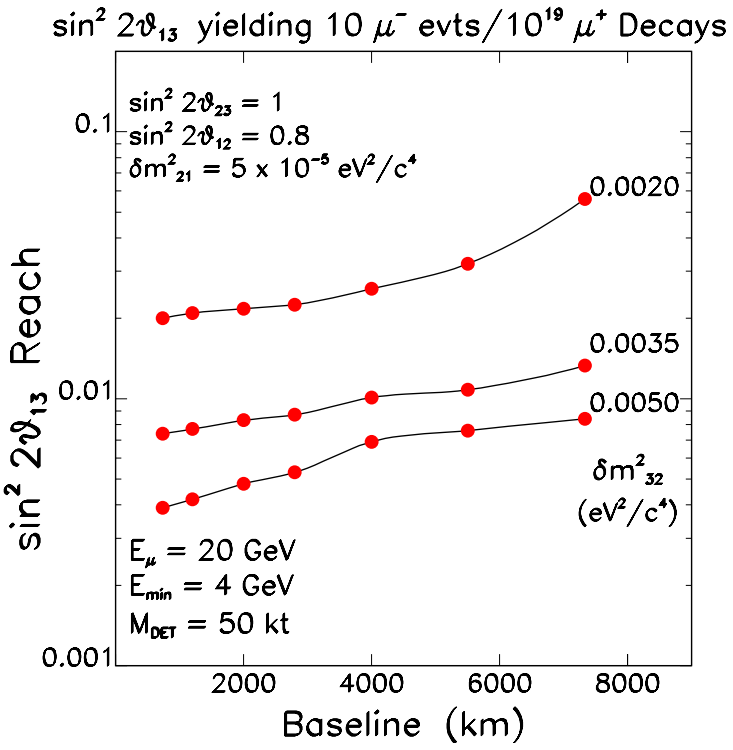

FIG. 3. Reach in $\sin^2 2\theta_{13}$ for the observation of 10 μ^- events from $\nu_e \to \nu_\mu$ oscillations, shown versus baseline for three values of δm^2_{32} spanning the favored SuperK range. The other oscillation parameters correspond to the LAM scenario in Table I. The curves correspond to $10^{19}\mu^+$ decays in a 20 GeV neutrino factory with a 50 kt detector, and a minimum muon detection threshold of 4 GeV.

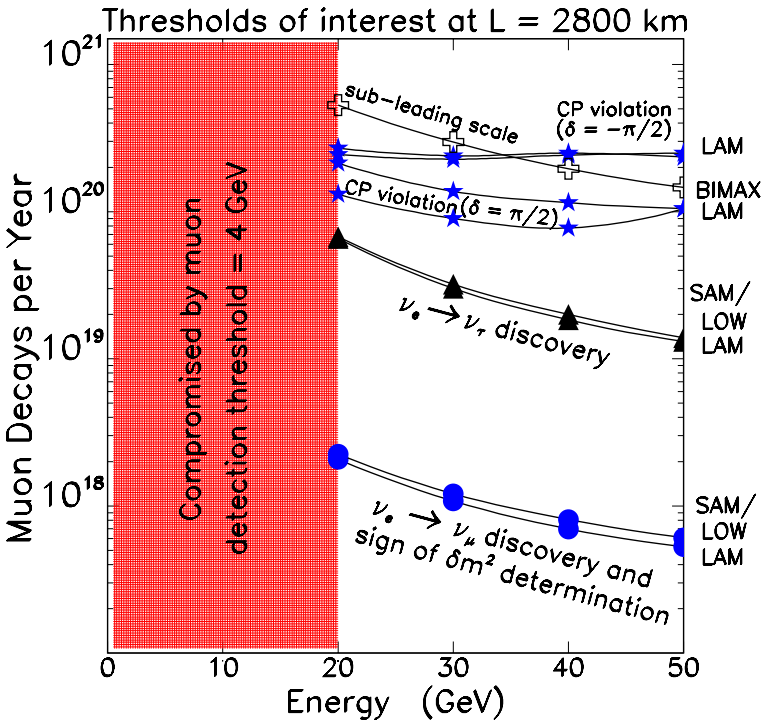

FIG. 4. The required number of muon decays needed in the beam-forming straight section of a neutrino factory to achieve the physics goals described in the text, shown as a function of storage ring energy for the scenarios listed in Table I. The baseline is taken to be 2800 km, and the detector is assumed to be a 50 kt wrong-sign muon appearance device with a muon detection threshold of 4 GeV or, for $\nu_e \to \nu_\tau$ appearance, a 5 kt detector.

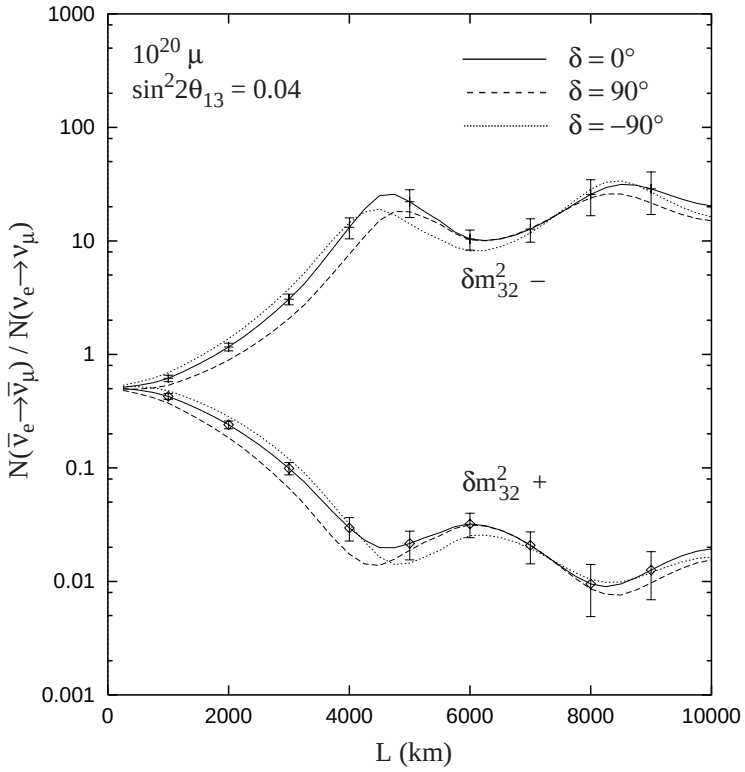

FIG. 5. The ratio R of $\bar{\nu}_e \to \bar{\nu}_\mu$ to $\nu_e \to \nu_\mu$ event rates at a 20 GeV neutrino factory for $\delta = 0$ and $\pm\pi/2$. The upper group of curves is for $\delta m^2_{32} < 0$, the lower group is for $\delta m^2_{32} > 0$, and the statistical errors correspond to 10^{20} muon decays of each sign and a 50 kt detector. The oscillation parameters correspond to the LAM solar solution with $|\delta m^2_{32}| = 3.5 \times 10^{-3}$ eV^2 and $\sin^2 2\theta_{13} = 0.04$.

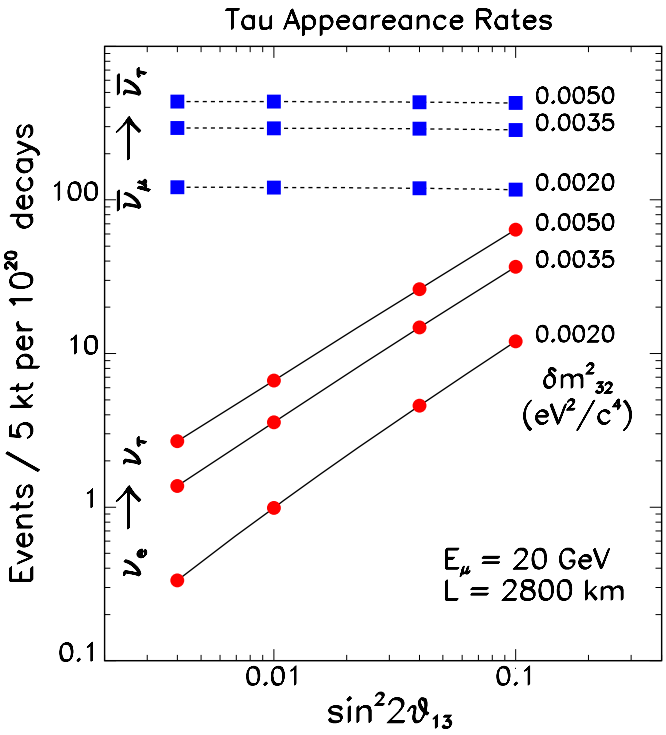

FIG. 6. τ CC appearance rates in a 5 kt detector 2800 km downstream of a 20 GeV neutrino factory in which there are $10^{20}\mu^+$ decays in the beam-forming straight section. The rates are shown as a function of $\sin^2 2\theta_{13}$ and δm^2_{32} with the other oscillation parameters corresponding to the LAM scenario in Table I. The top 3 curves are the predictions for $\bar{\nu}_\mu \to \bar{\nu}_\tau$ events and the lower curves are for $\nu_e \to \nu_\tau$ events.

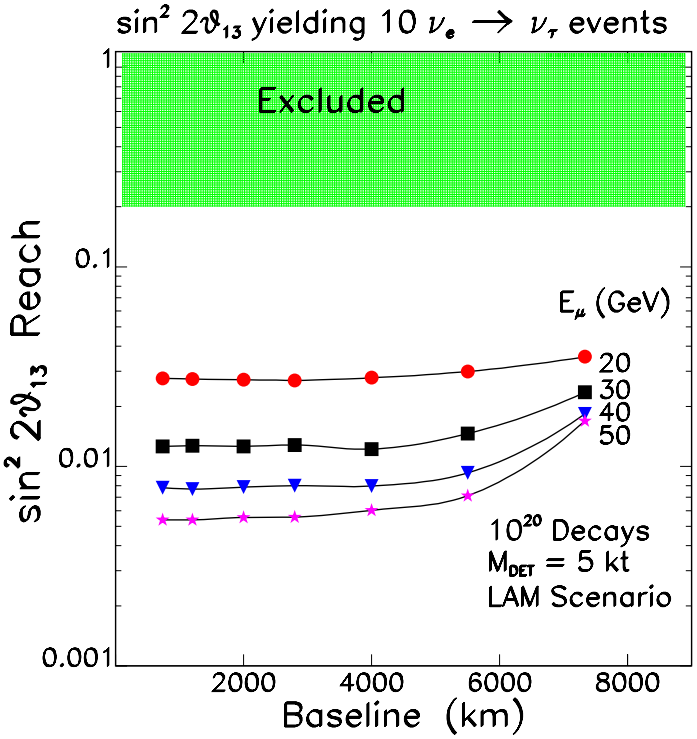

FIG. 7. Reach in $\sin^2 2\theta_{13}$ for the observation of 10 events from $\nu_e \to \nu_\tau$ oscillations, shown versus baseline for four storage ring energies. The oscillation parameters correspond to the LAM scenario in Table I. The curves correspond to 10^{20} μ^+ decays in a 20 GeV neutrino factory with a 5 kt detector.

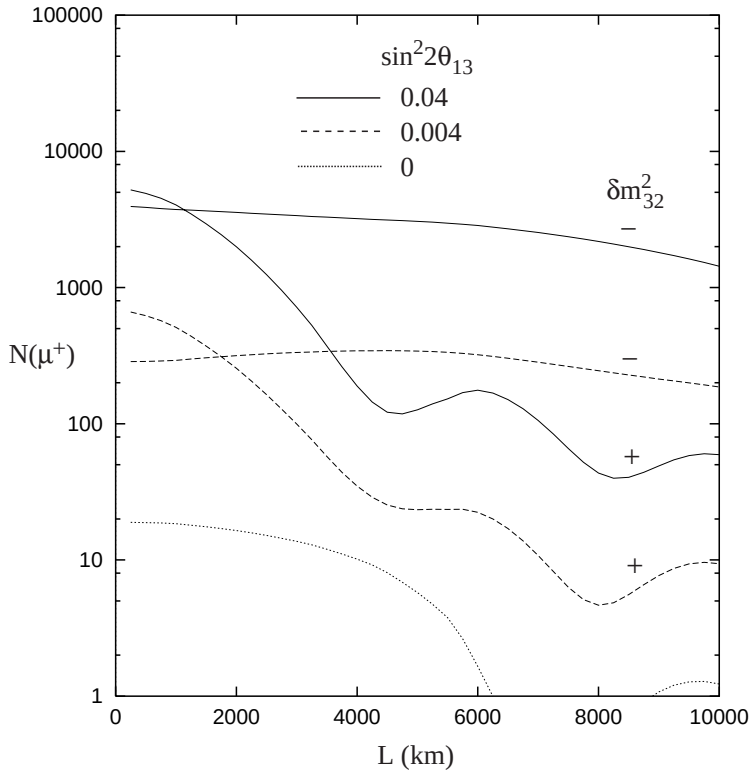

FIG. 8. The number of wrong-sign μ^+ CC events shown versus L, with $10^{21}\,\mu^-$, a 50 kt detector, and the LAM solar solution with $|\delta m^2_{32}| = 3.5 \times 10^{-3}$ eV^2 and $\delta = 0$, for the cases $\sin^2 2\theta_{13} = 0.04$ (solid curves), 0.004 (dashed), and 0 (dotted). Results for both signs of δm^2_{32} are shown.

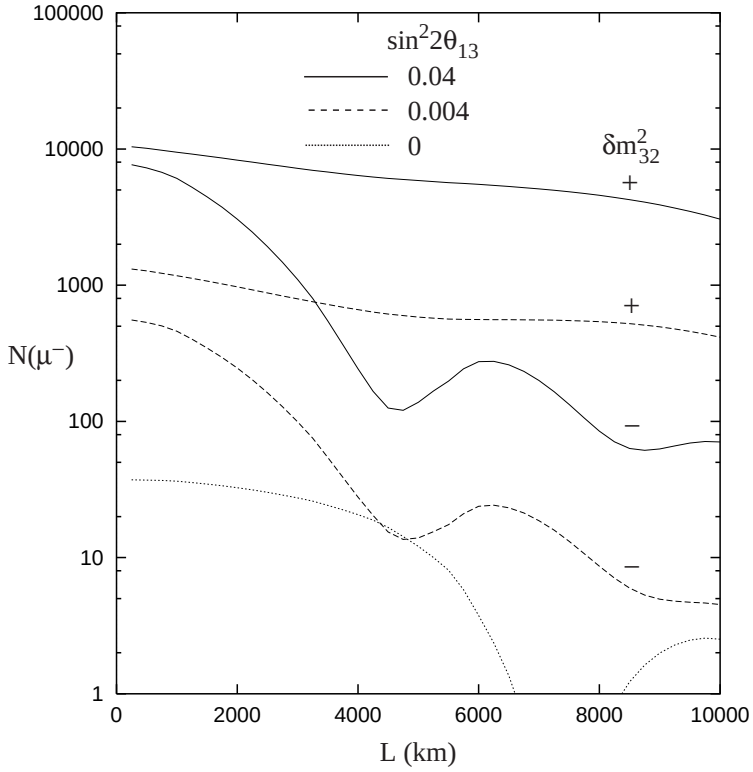

FIG. 9. The same as Fig. 8 for wrong sign μ^- events from a μ^+ beam.

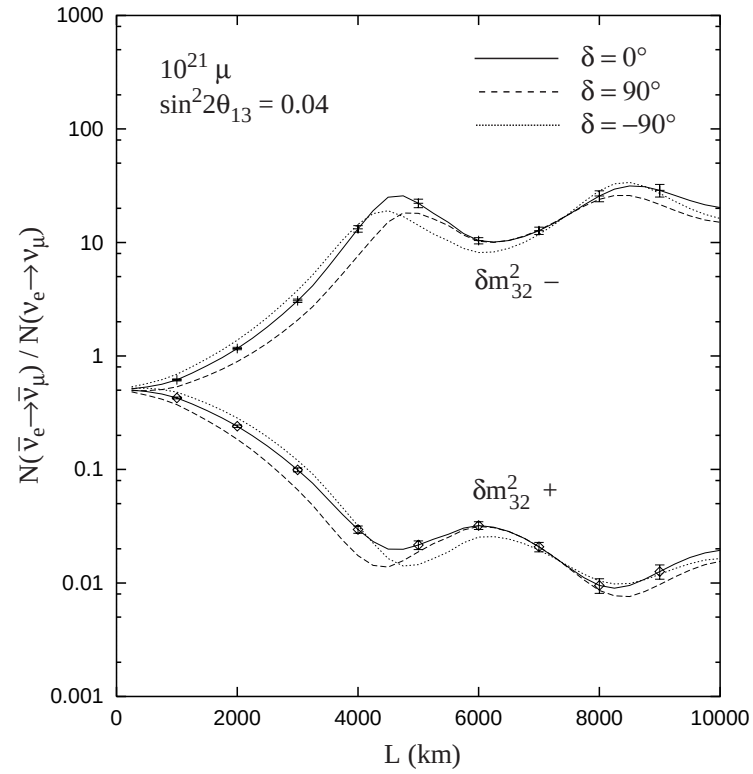

FIG. 10. Same as Fig. 5 except for 10^{21} muons.

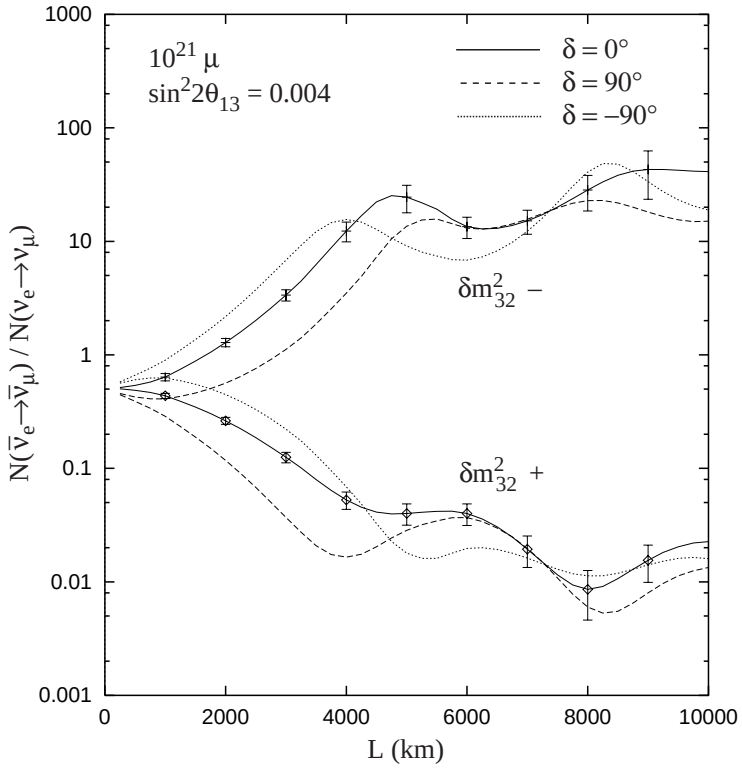

FIG. 11. Same as Fig. 5 except for 10^{21} muons and $\sin^2 2\theta_{13} = 0.004$.

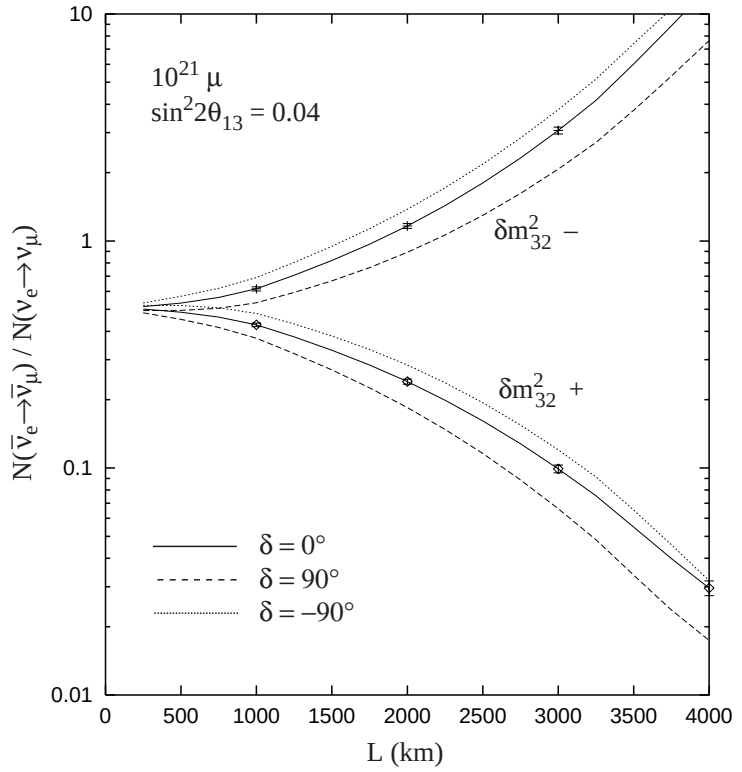

FIG. 12. Same as Fig. 10 for the range $0 \leq L \leq 4000$ km.

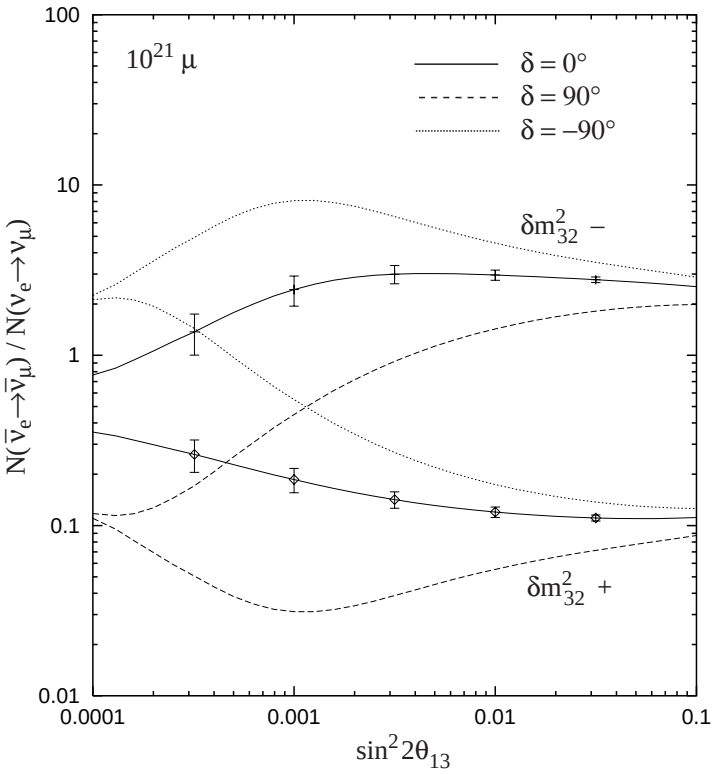

FIG. 13. The ratio of $\bar{\nu}_e \to \bar{\nu}_\mu$ to $\nu_e \to \nu_\mu$ CC events versus $\sin^2 2\theta_{13}$, with $L = 2900$ km, $E_\mu = 20$ GeV, 10^{21} muons, and a 50 kt detector. The other oscillation parameters are the same as the LAM scenario in Table I, and results for both positive and negative δm^2_{32} are shown. Predictions for maximal CP phases $\delta = 90°$ (dashed curves) and $\delta = -90°$ (dotted) are compared with the CP-conserving case $\delta = 0°$ (solid). The error bars show typical statistical uncertainties on the measurements.

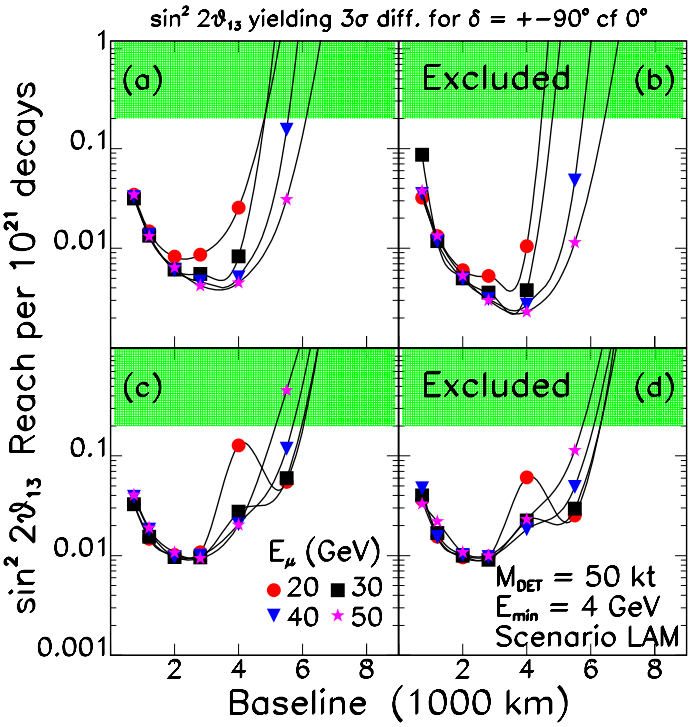

FIG. 14. Reach in $\sin^2 2\theta_{13}$ that yields a 3σ discrimination between (a) $\delta = 0$ and $\pi/2$ with $\delta m^2_{32} > 0$, (b) $\delta = 0$ and $\pi/2$ with $\delta m^2_{32} < 0$, (c) $\delta = 0$ and $-\pi/2$ with $\delta m^2_{32} > 0$, and (d) $\delta = 0$ and $-\pi/2$ with $\delta m^2_{32} < 0$. The discrimination is based on a comparison of wrong-sign muon CC event rates in a 50 kt detector when 10^{21} positive and negative muons alternately decay in the neutrino factory. The reach is shown versus baseline for four storage ring energies. The oscillation parameters correspond to the LAM scenario.